JACS
JOURNAL OF THE AMERICAN CHEMICAL SOCIETY

ARTICLE

pubs.acs.org/JACS

# Multiple Pathways of Dissociative Attachment: $CH_3Br$ on Si(100)-2×1

Ting Bin Lim,[†] Iain R. McNab,[†] John C. Polanyi,[*,†] Hong Guo,[‡] and Wei Ji[‡,§]

[†]Department of Chemistry and Institute of Optical Sciences, University of Toronto, 80 St. George Street, Toronto, Ontario M5S 3H6, Canada

[‡]Department of Physics, McGill University, Rutherford Building, 3600 rue University, Montréal (Québec) PQ H3A 2T8, Canada

Supporting Information

**ABSTRACT:** We describe the dissociative attachment (DA) of methyl bromide to form chemisorbed $CH_3$ and Br on a Si(100)-2×1 surface at 270 K. The patterns of DA were studied experimentally by ultra-high vacuum scanning tunneling microscopy (STM) and interpreted by ab initio theory. The parent molecules were found to dissociate thermally by breaking the C−Br bond, attaching the resulting fragments $CH_3$ and Br at adjacent Si-atom sites. The observed DA resulted in three distinct attachment geometries: inter-row (IR, 88%), inter-dimer (ID, 11%), and on-dimer (OD, 1%). Ab initio computation agreed in predicting these three DA reaction pathways, with yields decreasing down the series, in accord with experiment. The three computed physisorption geometries, each of which correlated with a preferred outcome, IR, ID, or OD, exhibited similar heats of adsorption, the choice of pathway being governed by the energy barriers to DA chemisorption predicted to increase along the series: $E_{IR} = 0.48$ eV, $E_{ID} = 0.57$ eV, and $E_{OD} = 0.63$ eV.

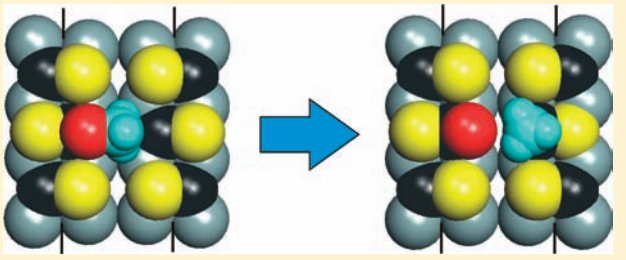

## INTRODUCTION

Among the most common categories of surface reaction is "single" dissociative attachment (DA) (also termed dissociative adsorption or dissociative chemisorption) in which a single bond in an adsorbate is severed and two new bonds attaching the fragments to the surface form. Since its introduction, STM has been employed in a number of instances to ascertain the outcome of DA on silicon surfaces.[1−12] Central to the understanding of the molecular dynamics of DA is knowledge of the preferred separations of the fragments, when chemically bound to the surface. However, even simple dissociative attachment is not yet well understood. Dissociative attachment is thought to occur through physisorbed precursor states of varying reactivity.[13] The principal mode for $H_2$ DA at Si(100)-2×1 is inter-dimer (ID),[11,12] although the bond length of $H_2$ is 0.74 Å, and the choice of final product separations is 2.7 Å for on-dimer (OD), 4.0 Å inter-dimer (ID), and 5.2 Å inter-row (IR). At the same surface, $Cl_2$, with a bond length of 1.99 Å, chemisorbs predominantly at substantially wider pair-separations, giving largely IR (52%) and, to diminishing extents, ID (33%) and OD (15%).[9] Simple polyatomic molecules, which undergo DA, have also been the subject of numerous experimental and theoretical studies to elucidate their reaction mechanisms and reaction outcomes;[1] $NH_3$ physisorbs by donation of electrons from N to Si and then undergoes DA at an N−H bond to give both OD and ID outcomes. The chemically similar $PH_3$ undergoes more complicated dissociative attachment reactions, giving a greater variety of dissociation products.[1] In this laboratory, we recently studied the DA of methyl chloride (C−Cl bond length 1.78 Å) at Si(100)-2×1, which gave almost exclusively IR DA,[10] and then, due to the mobility of physisorbed $CH_3Cl$, extended adsorbates into chains of alternating $CH_3$ and Cl chemisorbed on adjacent silicon dimer rows. Understanding of these varied findings in terms of ab initio theory remains at an early stage of development.

We observe three different pathways of DA for methyl bromide on Si(100)-2×1 (STM at 270 K). Using Density Functional Theory (DFT), we relate these three pathways to distinctive initial physisorbed states. The $CH_3Br$ molecule was found to undergo single dissociative attachment by breaking the C−Br bond, resulting in a $CH_3$-group and a Br-group, which both covalently attached to adjacent Si-atom sites at the surface. At room temperature, the initial distribution of chemisorbed Br from DA was obscured by migration of the Br to adjacent silicon atoms. We were, however, able to suppress this migration by working at a slightly reduced temperature of 270 K.

The three concurrent outcomes for $CH_3Br$ DA were characterized as IR, ID, and OD in conformity with terminology now widely used.[1]

Yates and co-workers,[9] who were the first to observe significantly multiple-pathway DA, suggested that the $\pi$-orbitals on the outer silicon atoms of adjacent silicon dimer-rows might interact most favorably with the molecular orbitals of a chlorine molecule physisorbed inter-row (IR; 5.2 Å). A progressively less-favorable overlap would apply to inter-dimer (ID; 4.0 Å) and on-dimer (OD; 2.7 Å) perhaps accounting for the declining probability for

**Received:** February 2, 2011
**Published:** June 22, 2011

these configurations with progressively higher dissociative attachment activation energies. Later, a quantum calculation of the effect of changing Si···Si dangling bond separation on the activation energy for dihalogenation evidenced this effect and predicted a most-favorable Si···Si separation of 3−4 Å greater than the interhalogen separation in the parent (*p*-dibromobenzene) molecule, lending weight to the Yates' group speculation that $Cl_2$ (1.99 Å in length) would encounter a minimum energy-barrier for inter-row reaction (IR; 5.2 Å).[14]

The present study provides, for the first time, a further example of multiple-pathway DA. The measured yields for the three pathways were predominantly IR (88%) followed by ID (11%) and OD (1%). In the present work, a more complete, albeit approximate, treatment by theory is given that has not been available until now for multiple-pathway DA. The theory was an ab initio DFT calculation (149 atoms, calculated with a 3 × 3 × 1 *k*-mesh) applied consistently to the initial physisorbed states and to the climbing image nudged elastic band calculation of the activation energies, to form the three DA products. Three physisorbed precursor states were found to predominate, each correlating with one of the observed outcomes. Methods of ab initio computation will improve over time, but three qualitative findings of the present work appear to be significant: first that physisorbed precursor states exist, which have distinctive geometries plausibly correlating with the three DA outcomes, second that their physisorption energies are, in the present case, similar, and third that the observed preference for inter-row (IR) over inter-dimer (ID), which in turn is preferred to on-dimer (OD), has to do with a progressive increase in activation barrier in going from IR to ID to OD.

## EXPERIMENTAL METHOD

All experiments were carried out in ultrahigh vacuum with an Omicron scanning tunneling microscope (VT-STM, base pressure of $1.5 \times 10^{-10}$ Torr). Images were obtained in constant current mode, with a set-point of 0.2 nA. Single crystal Si(100) samples were cut from 6 in. Si(100) wafers obtained from Virginia Semiconductors (n-type, P-doped, 0.02 Ω cm) using a diamond scribe. The Si samples were cleaned in the vacuum chamber using direct current heating to temperatures of around 1200 °C for periods of 30 or 60 s. The temperatures reached by the samples were measured using an optical pyrometer (Cyclops 152, Minolta), with an emissivity setting of 0.63. Before each experiment, the samples were subject to eight such flashing periods, each 5 min apart, before a final short 5 s flash followed by a slow ramp-down of the heating current (0.1 A per 20 s) to bring the temperature of the sample gradually from a temperature of around 960 °C to room temperature.

To cool the samples on the STM stage to a temperature of about 270 K, cold dry nitrogen gas was passed through the STM cryostat. The nitrogen was cooled by passing it through a coil of copper tubing immersed in a bath of liquid argon. As liquid argon has a boiling point above that of liquid nitrogen, the nitrogen gas was cooled without being condensed to liquid. We found this arrangement gave sufficient cooling without introducing vibration to the STM stage. Fine temperature control was achieved by counterheating the cryostat using a Lakeshore 331 temperature controller. Typically, the temperature was stable to 1 K over a few hours. Before exposure to $CH_3Br$, the cooled silicon surface was checked by STM and found to have contamination from background adsorption of <0.3%. Imaging of the cooled surface took place within 1 h following the dose of $CH_3Br$, during which time no further contamination of the surface became evident.

Methyl bromide gas from Aldrich ($CH_3Br$, 99.5+%, CAS number 74-83-9) was introduced into the vacuum chamber through a leak-valve. Dosing was monitored by an ion gauge in the same chamber. The gas line was typically flushed 7−8 times with $CH_3Br$ before dosing. For each exposure, the nominal dose was recorded in Langmuir (L) from the dosing pressure of the $CH_3Br$ (as measured at an uncorrected ion gauge) multiplied by the time of the exposure in seconds (1 L = $10^{-6}$ Torr s). Corrected pressures (and therefore doses) would be about 2.5 times lower.[15]

Initial state physisorption geometries of $CH_3Br$ adsorbed on Si(100)-2×1 were calculated ab initio using DFT, using the Perdew−Burke−Ernzerhof (PBE) generalized-gradient approximation (GGA) for exchange-correlation potentials, the projector augmented waves (PAW) method, and a plane-wave basis set of 400 eV, as implemented in the Vienna ab initio simulation package (VASP). A 4 × 4 supercell was used consisting of seven layers of Si atoms, terminated at the bottom with 32 valence H-atoms. The adsorbate molecule was put on the top face of the slab. The surface Brillouin-zone was sampled using a 3 × 3 × 1 *k*-mesh, and calculations were performed with spin-polarization applied. The bottom three layers of silicon atoms were frozen, and all other atoms were fully relaxed until the net force on every atom was less than 0.02 eV/Å.

The potential-energy profiles along the reaction paths were calculated by VASP using the climbing image nudged elastic band (CI-NEB) technique,[16] which located the saddle points of the reactions.

## RESULTS AND DISCUSSION

Initial observations of methyl bromide on Si(100)-2×1 were made at room temperature (see below). Before the surface was observed, all intact methyl bromide had either dissociatively attached or desorbed. Initially during imaging at 300 K, we observed Br-migration on the surface. In subsequent work, this was suppressed by dosing and imaging the surface at the slightly reduced temperature of 270 K.

**Dissociative Attachment of $CH_3Br$ on Si(100)-2×1 at 270 K (Figure 1).** The 270 K silicon surface was dosed with 0.3 L (60 s at $5 \times 10^{-9}$ Torr) of $CH_3Br$. A typical negative surface bias STM image of the resulting patterns of DA is shown in Figure 1. All $CH_3Br$ molecules reacted thermally before imaging. The three main surface features due to the reaction products of $CH_3Br$ molecules are identified on the image; they are labeled OD, ID, and IR on the basis of their geometries on the surface.[1] The relative yields of each product type are also given in the figure, based on an analysis of 104 single-molecule reaction features at 270 K.

The OD, ID, and IR products all consist of two moieties, $CH_3$(ad) and Br(ad), bonded covalently onto either a single Si dimer-pair (OD), two Si dimer-pairs of the same dimer row (ID), and two Si dimer-pairs of adjacent dimer rows (IR). The silicon atoms with chemisorbed adduct are darkened in the negative surface bias STM images, as can be seen most clearly for the OD product. In ID and IR products, each of which involve two Si dimer-pairs, the other silicon atoms of the dimer-pair, not directly involved in bonding, become a dangling bond (labeled DB). These DB's can be seen to be brighter than the normal Si-dimer atoms of the rest of the surface, at the sample bias shown (−1 V s).

The assignment of the chemisorbed pairs of reaction products to OD, ID, or IR is given in Figure 1. The assignment is based on the appearance of the products at different sample biases. At sample biases of around +2.4 $V_{surf}$, the Br atoms bonded to Si atoms appear higher than the clean Si dimer-pair atoms in the topographical image[17] due to a localized increase in density of states resulting from the Br−Si bonding. This allows us to

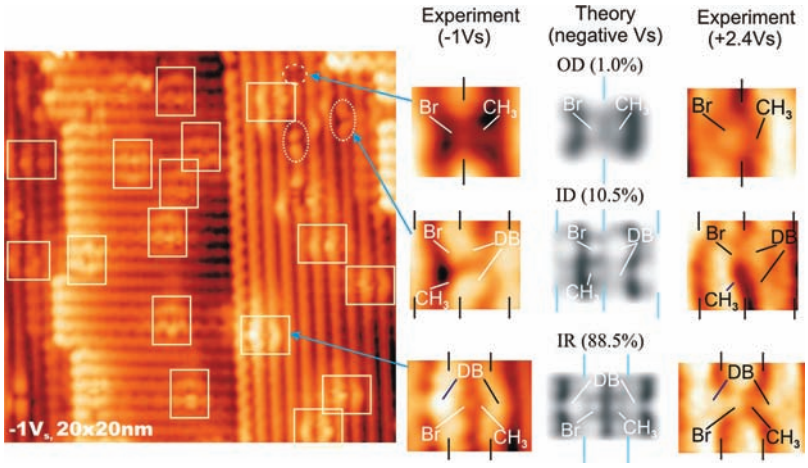


**Figure 1.** STM image showing the outcome of dissociative attachment of methyl bromide at a cooled (270 K) Si(100)-2×1 surface. Three distinguishable outcomes of DA are identified: on-dimer (OD), inter-dimer (ID), and inter-row (IR). Close-up STM images are compared to theoretically simulated images to the right of the main image.

determine which of the darkened products at −1 $V_{surf}$ sample bias are the Br-atoms, and consequently which are $CH_3$ groups. For the main reaction-product, IR, we have further confirmed this assignment by the observation of significant thermal hopping (observed $k_{hop}$ = 8.62 × $10^{-4}$ $s^{-1}$ at 270 K) by individual Br-atoms between the two Si-atoms of a single silicon-dimer. No such hopping was observed for the $CH_3$ group in the IR products, a process that we calculated to have a higher energy-barrier [1.3 eV, cf., 0.4 eV for Br]. This Br-atom hopping process also accounts for the different appearance of some of the boxed IR products in Figure 1, where the bright dangling bond seems to be between the silicon-dimer rows instead of at the end.

In no cases did the STM images at 270 K yield an isolated Br-atom or $CH_3$-group. Even in experiments at very low surface-coverage, pairs of $CH_3$(ad) and Br(ad) groups were exclusively observed in all of the OD, ID, and IR configurations. This is consistent with each pair of reaction products coming from the same parent molecule $CH_3Br$, with the result that both fragments stay bonded to the surface after the molecule breaks up in dissociative attachment (DA). There is no evidence of the "abstraction" of a single $CH_3$ or Br by this surface from the parent molecule, in the temperature range of 270−300 K examined.

The relative experimental yields of DA shown in Figure 1 for 270 K vary markedly. From a total of 104 species counted, the proportions are OD (<1.0%; 1 count), ID (10.5 ± 3.2%; 11 counts), and IR (88.5 ± 9.2%; 92 counts). Assuming Arrhenius behavior and the same pre-exponential factors for the rate constants of each reaction pathway, the ratio of any two relative yields provides the difference in activation energies between the two pathways. This is summarized in Table 1in the "$\Delta E_a$ expt" column. As we have only one example of an OD species in this case, we are only able to determine a lower limit for the difference in activation energies.

**Migration Br on Si(100)-2×1 at 300 K.** STM following dosing of $CH_3Br$ on Si(100)-2×1 at room temperature (300 K) showed a dependence of the image on the time between dosing and scanning. Images taken over a period of several hours showed that the adsorbed species that we identify as chemisorbed Br were migrating across the surface moving between adjacent Si dimer-pairs of a Si dimer-row. This phenomenon was not observed in the measurements made at 270 K. This migration makes the analysis of room temperature images unsuitable for understanding the initial pattern of reaction of $CH_3Br$ on this surface.

**Table 1. Differences between Activation Energies for Observed Reaction Outcomes, As Derived from the Experimental Observation of the Relative Yields of the Three Reaction Outcomes, As Compared to ab Initio Values Obtained by the Climbing Image Nudged Elastic Band Technique, Implemented in VASP**

| pathways compared | $\Delta E_a$ expt | $\Delta E_b$ theory |
|---|---|---|
| ID/IR | 0.05 ± 0.01 eV | 0.08 eV |
| OD/IR | ≥0.10 eV | 0.14 eV |

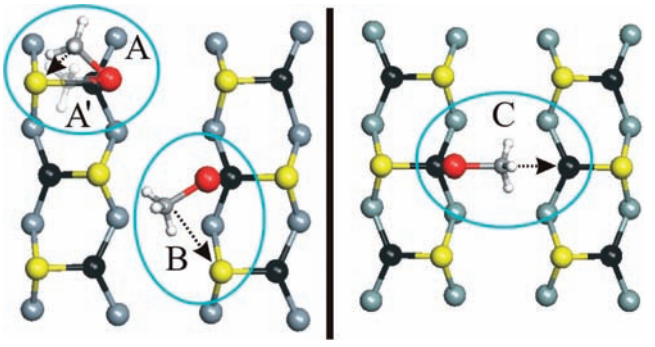


**Figure 2.** Calculated physisorption geometries for the $CH_3Br$ molecule on Si(100)-p(2×2) (at left) and Si(100)-c(4×2) (at right). [See Figure 3 for side views.] Blue ovals enclose the physisorbed states. The dotted arrows show the destination of the $CH_3$ groups upon dissociative attachment.

We quantified the experimental migration rate of Br(ad) along the Si dimer-pair row by tracing the same dosed area at times longer than an hour apart at 280 K. The main mode of migration of Br(ad) was by jumping along a single silicon-dimer row, from one silicon-dimer to an adjacent one. The rate constant was measured as $k_{mig}$ = (7.9 ± 3.3) × $10^{-6}$ $s^{-1}$. Assuming Arrhenius behavior, and a pre-exponential constant between $10^{11}$ and $10^{15}$ $s^{-1}$, this gives an experimental barrier to migration of

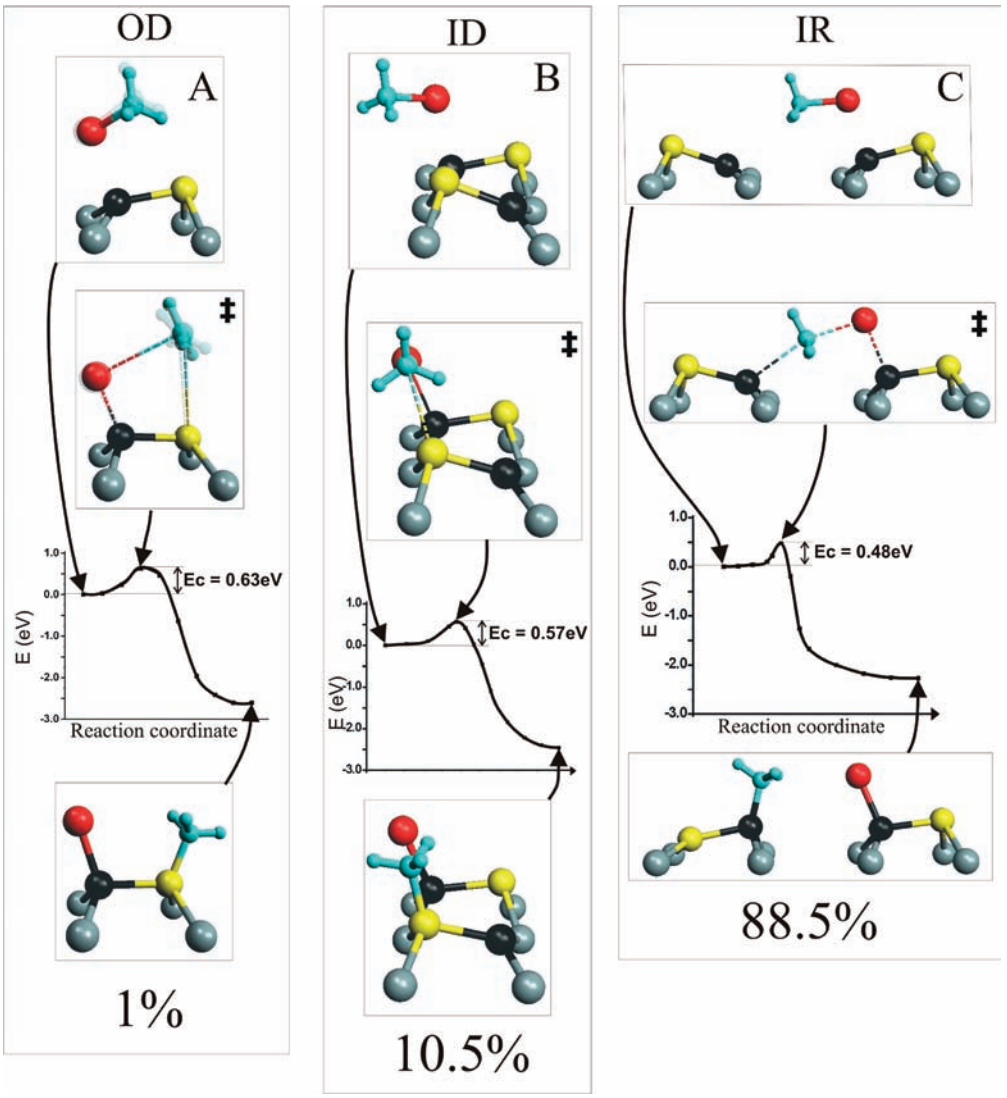


**Figure 3.** Physisorption geometries correlated with outcomes of dissociative attachment. Four physisorption geometries are found from theory (A, A′, B, and C). The lowest energy reactive pathway for each physisorption geometry correlated with the three observed outcomes of dissociative attachment (OD, ID, IR). The initial states, transition states, reaction coordinate, and final outcomes of dissociative attachment are shown for each of OD, ID, and IR, in each of the three vertical columns. In the OD column physisorbed state, A is shown clearly, while A′ is a faint outline. The percentage yields are those observed experimentally at 270 K.

$E_{mig}$(expt) = 1.0 ± 0.1 eV. We have also computed the migration barriers for Br on this surface ab initio and found inter-dimer migration barriers along the Si-dimer row $E_{mig}$(theory) = 0.77−0.91 eV, depending on the buckling configuration of the surface Si-dimers used (see the Supporting Information). Theory is in excellent agreement with experiment.

**Computed Physisorption Configurations.** To find suitable starting points for modeling the observed DA reaction pathways, calculations were made using ab initio theory to find the most stable physisorbed configurations of intact $CH_3Br$ molecules on this surface. Although the experimental surface has a dynamic flipping of Si-dimers, the simulations suppress this flipping. The two most stable frozen configurations of Si(100), Si(100)-c(4×2) and Si(100)-p(2×2), were both considered as substrates for physisorption.

Figure 2 shows the three categories of adsorption geometry (A, B, and C) for intact physisorbed $CH_3Br$ on the Si(100)-p(2×2) and Si(100)-c(4×2) surfaces, obtained from ab initio DFT calculations. The three physisorbed geometries have comparable heat of adsorption, ∼−0.40 eV. Type A is accompanied by a fourth physisorption state, A′, with a heat of adsorption of −0.37 eV. A′ differs from A in having the $CH_3$ group more closely aligned with the silicon with which it will bind in OD reaction. The Br positions for A and A′ are the same. All of the physisorbed states have the Br end of the molecule positioned above a "down" Si atom of a silicon dimer-pair ($Si_d$, black in the figure). The "down" Si-atom in a dimer is known to be slightly positive with respect to the "up" atom of the same Si-dimer pair, due to charge transfer.[18] The preference of Br for the "down" atom is likely to be due to dative bonding from Br in $CH_3Br$ to a $Si_d$ atom. This dative interaction has also been invoked for physisorbed precursor states of other simple polar molecules such as $NH_3$ and $PH_3$ on this surface.[19] Figure 2 shows that in category A the $CH_3Br$ is approximately over a Si dimer-pair (OD physisorption), in category B physisorption involves adjacent dimer-pairs of one row (ID), and in category C it involves adjacent dimer-pairs of

two different rows (IR). The main difference between the three physisorbed configurations is the orientation of the C−Br bond axis with respect to the surface. Significantly, this C−Br bond direction has consequences for the preferred reaction pathway from each physisorbed state, as illustrated below from nudged elastic band (NEB).

**Computed Energy Profiles and Barrier Heights for DA Reaction.** Energy profiles were calculated for dissociative attachment, using the NEB method and DFT, starting from each of three physisorption states and terminating in final states of OD, ID, or IR based on the geometry of the physisorbed molecule. The lowest computed barrier-height, $E_c$, measured relative to the physisorbed molecule's potential-well minimum for each type of DA (OD, ID, and IR) was used as the value for that DA pathway. Other barrier heights are reported in the Supporting Information. In Figure 3, the three reaction energy profiles are shown. For each energy profile, molecular models are shown for the initial state (labeled A, A', B, or C, as in Figure 2), the transition state (marked by a "‡" sign), and the final state.

Each of the three physisorption states exhibits a low energy barrier, $E_c$, for reaction to a single observed outcome: OD, ID, or IR. For the major pathway, IR, the observed outcome is a consequence of the inter-row location of the physisorbed molecule. Because all of the physisorption states have the Br group over a "down" Si-atom site, this is the Si with which Br reacts. The $CH_3$ binds to the silicon to which the $H_3C-Br$ bond-axis points.

The calculations produced $E_c$ values in quantitative agreement with the experimentally observed yields of DA at 270 K: OD (1.0%) has the highest barrier, followed by ID (10.5%), and then IR (88.5%). The differences in calculated barrier height, $\Delta E_c$, between the different pathways agreed with the differences in the derived interaction energies $\Delta E_a$, from the experimental yields of OD, ID, and IR; see Table 1.

Theory and experiment are in accord in the calculated and measured dissociative sticking probabilities. We computed the dissociative sticking probability, $p$, using the thermally trapped physisorbed precursor model of Weinberg,[20] in which $p$ = (trapping probability) × $[k_r/(k_r + k_d)]$, where $k_r$ and $k_d$ are the thermal rate constants for reaction and desorption. The trapping probability is taken as unity based on the measurement for $CH_3Cl$ on the same surface at room temperature.[21] The rate constants were calculated from Arrhenius expressions using the computed reaction barrier (0.48 eV) and physisorption energy (0.41 eV) for the major reaction pathway, IR. Assuming the two rate constants to have the same $A$-factor, we have $p \approx 5 \times 10^{-2}$. From our experimental impingement rates, dosing time, and observed coverage, we obtained $p \approx 8 \times 10^{-2}$, in good agreement with the calculated $p$ value from DFT theory. This agreement indicates that the DFT calculation is a reasonable approximation for this system.

## CONCLUSION

The dissociative attachment reaction pathways available to a $CH_3Br$ molecule with the Si(100)-2×1 surface at 270 K have been obtained experimentally by STM and have been computed by ab initio theory. Measurement of the yields of individual reaction-product atoms and radicals, Br and $CH_3$, gave the relative ordering of the energy barriers for the three categories of dissociative attachment, in order of decreasing yields IR, ID, and OD (inter-row, inter-dimer, and on-dimer), as well as differences in barrier heights. At room temperature, migration of the Br groups after initial DA was observed and measured.

Ab initio computations indicated that $CH_3Br$(ad) molecules physisorb in three different geometries on this surface, each of which leads preferentially to a specific reaction outcome: IR, ID, or OD. Qualitative agreement was found between experimentally deduced and computed ordering of reaction energy barriers, as well as agreement between experimental and computed differences between the reaction energy barriers, to give the three observed outcomes of dissociative attachment.

## ASSOCIATED CONTENT

**Supporting Information.** Additional minor reaction pathway and barrier height. This material is available free of charge via the Internet at http://pubs.acs.org.

## AUTHOR INFORMATION

**Corresponding Author**
jpolanyi@chem.utoronto.ca

**Present Addresses**
[§]Department of Physics, Renmin University of China, 59 Zhongguancun Ave, Beijing 100872, China.

## ACKNOWLEDGMENT

J.C.P. and H.G. are grateful for financial support from the Natural Sciences and Engineering Research Council of Canada (NSERC) and Canadian Institute for Advanced Research (CIfAR). J.C.P. also thanks Photonics Research Ontario (PRO) an Ontario Centre of Excellence and the Xerox Research Centre Canada (XRCC) for financial support. W.J. thanks NSFC (Grant No. 11004244) of China and BNSF (Grant No. 2112019) of Beijing for financial support.

## REFERENCES

(1) Owen, J. H. G. *J. Phys.: Condens. Matter* **2009**, *21*, 443001.
(2) Queeney, K. T.; Chabal, Y. J.; Raghavachari, K. *J. Chem. Phys.* **2003**, *119*, 2307–2313.
(3) Ranke, W. *Surf. Sci.* **1996**, *369*, 137–145.
(4) Konecny, R.; Doren, D. J. *J. Chem. Phys.* **1997**, *106*, 2426–2435.
(5) Yu, S.; Kim, H.; Koo, J. *Phys. Rev. Lett.* **2008**, *100*, 036107.
(6) Chung, O. N.; Kim, H.; Chung, S.; Koo, J. *Phys. Rev. B* **2006**, *73*, 033303.
(7) Owen, J. H. G.; Bowler, D. R.; Kusano, S.; Miki, K. *Phys. Rev. B* **2005**, *72*, 113304.
(8) Bowler, D. R.; Owen, J. H. G. *Phys. Rev. B* **2007**, *75*, 155310.
(9) Lyubinetsky, I.; Dohnalek, Z.; Choyke, W. J.; Yates, J. T., Jr. *Phys. Rev. B* **1998**, *58*, 7950.
(10) Lim, T.; Polanyi, J. C.; Guo, H.; Ji, W. *Nat. Chem.* **2011**, *3*, 85.
(11) Dürr, M.; Höfer, U. *Surf. Sci. Rep.* **2006**, *61*, 465.
(12) Brenig, W.; Pehlke, E. *Prog. Surf. Sci.* **2008**, *83*, 263.
(13) De Pristo, A. E. In *Dynamics of Gas−-Surface Interactions*; Rettner, C. T., Ashfold, M. N. R., Eds.; The Royal Society of Chemistry: Cambridge, 1991; p 47.
(14) Matta, C. F.; Polanyi, J. C. *Philos. Trans. R. Soc., A* **2004**, *362*, 1185–1194.
(15) Bartmess, J. E.; Georgiadis, R. M. *Vacuum* **1983**, *33*, 149–153.
(16) Henkelman, G.; Uberuaga, B. P.; Jonsson, H. *J. Chem. Phys.* **2000**, *113*, 9901.

(17) Koji, W.; Nakayama, S.; Sugano, T.; Ohmori, K.; Signor, A. W.; Weaver, J. H. *Surf. Sci.* **2006**, *600*, 716–723.
(18) Toshinobu, J. *Chem. Rev.* **2004**, *77*, 37–70.
(19) Filler, M. A.; Bent, S. F. *Prog. Surf. Sci.* **2003**, *73*, 1–56.
(20) Weinberg, W. H. Kinetics of Surface Interactions. In *Dynamics of Gas—Surface Interactions*; Rettner, C. T., Ashfold, M. N. R., Eds.; The Royal Society of Chemistry: Cambridge, 1991; pp 171—219.
(21) Woelke, A.; Imanaka, S.; Watanabe, S.; Goto, S.; Hashinokuchi, M.; Okada, M.; Kasai, T. *J. Electron Microsc.* **2003**, *54*, i21–i24.